ISSN: 0975-833X

Available online at http://www.journalcra.com

International Journal of Current Research
Vol. 8, Issue, 03, pp.28000-28006, March, 2016

INTERNATIONAL JOURNAL OF CURRENT RESEARCH

RESEARCH ARTICLE

FOLIC ACID-GELATIN COATED HAp@Al_2O_3 CORE-SHELL NPs FOR RECEPTOR-MEDIATED TARGETED DRUG DELIVERY SYSTEM

Ramesh, I. and *Meena, K. S.

Department of Chemistry, Queen Mary's College, Chennai, Tamilnadu, India

ARTICLE INFO

Article History:
Received 18th December, 2015
Received in revised form
26th January, 2016
Accepted 15th February, 2016
Published online 16th March, 2016

Key words:
Ceramic nanoparticles,
Targeted drug delivery.
Folate receptors,
5-fluorouracil.

ABSTRACT

The hydroxyapatite (HAp) NPs was synthesized by co-precipitation method and Al_2O_3 shell was coated by sonochemical process. Gelatine(GEL) and folic acid(FA) are attached onto the nanoparticles utilizing different techniques. HAp@Al_2O_3-gelatin-folic acid (HAp@Al_2O_3-GEL-FA) core-shell nanostructures were characterized by FTIR, XRD, and HR-TEM techniques. The incorporation of gelatin-folic acid onto HAp@Al_2O_3 NPs exhibited good water dispersibility, enhanced drug delivery efficiency, and remarkable targeting ability to cancer cells. 5-fluorouracil (5-Flu) was used as a model drug. The in-vitro drug release of HAp@Al_2O_3-gelatin-folic acid NPs was studied at different pH conditions (7.4 and 6.3). Cytotoxicity of free HAp@Al_2O_3-GEL-FA NPs, free 5-Flu, and 5-Flu loaded former NPs was investigated against ovarian cancer cell line (SKOV3). The results shown that the 5-Flu loaded HAp@Al_2O_3-gelatin-folic acid NPs show greater cytotoxicity due to the folate receptor- over expressing in cancer cells. The present findings show that 5-Flu loaded gelatin-folic acid incorporated HAp@Al_2O_3 core-shell nanoparticles are promising for receptor-mediated targeted drug delivery system.

Citation: Ramesh, I. and Meena, K. S. 2016. "Folic acid-gelatin coated HAp@Al_2O_3 core-shell NPs for receptor-mediated targeted drug delivery system", *International Journal of Current Research,* 8, (03), 28000-28006.

INTRODUCTION

Cancer is regarded as one of the frightful diseases. Despites the development in the theranostics of cancer, the cure rate for this dreadful disease without any side effect is elusive (Shixian *et al*., 2013). As surgery and radiation therapy may not possible at advanced stages of cancer, chemotherapy is commonly preferred. A chemotherapeutic approach is highly significant in the treatment of solid tumors, but most of the available anticancer drugs damage the normal tissue and create systemic toxicity relating to severe side effects. Among various chemotherapeutic agents, were used in the treatment of various cancers. 5-fluorouracil (5-Flu) is one of the most commonly used chemotherapeutic agents for human malignancies (Daniele *et al*., 2013). In recent years, nanoparticles (NPs) with controlled phase, shape, and size have been extensively used in biomedical applications for imaging, drug delivery, and gene therapy (Dubertret *et al*., 2002; Nam *et al*., 2003; Jin *et al*., 2010; Veiseh *et al*., 2010; Wang *et al*., 2010). Ceramics nanoparticles already have been widely used in a broad spectrum of biomedical applications, and now drug delivery is. one of the fastest emerging and developing arenas for nano-ceramics, drawing increasing attention over the past few years Hydroxyapatite (HAp) has been widely accepted in the biomedical industry for orthopaedics, maxillofacial surgery and dental implants because of its biocompatibility and osseous integration (Wang *et al*., 2005). HAp has achieved excellent results as bioceramics in bone-substituted operations and in teeth repair due to its unique mechanical properties and bioactivity (Wang *et al*., 2005; Capriotti *et al*., 2007; Zhou and Lee, 2011). However its clinical applicability is restricted due to its poor mechanical strength (Zhou and Lee, 2011). Hence, there is a need to improve the mechanical properties of the HAp coatings without compromising the biocompatibility. Several research studies are being undertaken to overcome this limitation by preparing nanocomposites with reinforcing polymers, metal oxides and strong bioceramics (Itokawa *et al*., 2007; Mohamed *et al*., 2013; Kantana *et al*., 2013). Despite the advantages that HAp presents, the brittle nature, and low fracture toughness of HAp coating often result in rapid wear, and premature fracture of the coated layer. Inorganic metal oxide nanoparticles can be used as effective weapon for biomedical applications, due to its stability and biocompatibility properties (Gordon *et al*., 2011). As a response to such need, many efforts have attempted to enhance the mechanical properties of HAp via the addition of secondary ceramic reinforcement materials such as Al_2O_3, ZrO_2, and TiO_2

Corresponding author: Meena, K. S.
Department of Chemistry, Queen Mary's College, Chennai, Tamilnadu, India.

(Fu *et al*., 2002; Im *et al*., 2007; Li *et al*., 1995; Inuzuka *et al*., 2004; Singh *et al*., 2006; Evis and Doremus, 2007; Gautier *et al*., 1997; Evis *et al*., 2005; He *et al*., 2004). Al_2O_3 has a variety of commercial and industrial uses and is one of the most important commercial ceramic materials (Uyeda, 1991). Al_2O_3-NPs also have biological applications such as biosensors (Liu *et al*., 2011), bio filtration and drug delivery (Monteiro-Riviere *et al*., 2010), antigen delivery for immunization purposes (Skwarczynski and Toth, 2011), and bactericides (Sadiq *et al*., 2009; Ansari *et al*., 2013; Ansari *et al*., 2014b). Alumina coatings have been widely used for anti-wear and anticorrosion applications due to their high hardness, chemical inertness and high melting point, as well as to their high resistance to abrasion and erosion (Mindivan *et al*., 2009; Rico *et al*., 2013). Although Al_2O_3 coatings are selected for their favourable mechanical properties, they do not meet the requirement of drug delivery behaviour, which has limited their application in microbiologically influenced corrosion, water treatment industry and environmental protection etc. Therefore, considerable efforts have been made to develop the drug delivery system of Al_2O_3 coatings (Pisarek *et al*., 2013; Fajardo *et al*., 2014). Al_2O_3 coatings could be prepared by techniques such as chemical vapour deposition (CVD), physical vapour deposition (PVD), sol–gel, plasma electrolytic oxidation (PEO) and plasma spray (Guidi *et al*., 2005). Gelatin is a protein derived from collagen and commonly used plasma expander. Some of the useful properties of gelatin include solubility, biodegradability, biocompatibility and pH induced surface charge (Young *et al*., 2005). Presence of multifunctional groups, like –NH2, –COOH, in the gelatin chain makes it a suitable candidate to bind with anticancer drugs (Leo *et al*., 1997). The targeting of cancer cells can be achieved by means of conjugation of specific ligands to the probe. Folic acid (FA) has been widely used as a ligand because the folate receptor (FR) were over expressed in many types of cancer cells, but not in normal tissues (Leo *et al*., 1997; Sudimack and Lee, 2000; Zhang *et al*., 2002). Therefore, FA-mediated delivery should be an effective way for targeted drug delivery system. In this paper, we were prepared 5-fluorouracil loaded HAp@Al_2O_3-GEL-FA nanoparticles, and the structure were analysed by FTIR, HR-TEM, XRD, techniques. The cytotoxcity of HAp@Al_2O_3-GEL-FA nanoparticles were investigated against SKOV3cell lines by folate-receptor-mediated endocytosis.

Experimental section

Chemicals

Special grade reagents calciumnitrate tetrahydrate ($Ca(NO_3)_2$ $4H_2O$), diammonium hydrogen phosphate ($(NH_4)_2HPO_4$), aluminium isopropoxide were purchased from Sigma Aldrich (USA). All other chemicals used were of analar grade. Milli-Q water was used in all the synthesis.

Synthesis of HAp NPs

The HAp NPs was prepared by slight modification of the method described in the literature (Bouyer *et al*., 2000). Briefly, 1 M of $Ca(NO_3)_2$ $4H_2O$ and 0.6 M of $(NH_4)_2HPO_4$ were dissolved in Milli-Q water separately. The pH of both aqueous solutions was brought to 11 by using 25% of NH_4OH solution under vigorous stirring the Ca $(NO_3)_2$ $4H_2O$ was added drop wise to $(NH_4)_2HPO_4$ solution over a period of 1 h to produce a milky white precipitate, which was then stirred for 1 h. Then the reflux process was carried out at 100 ^{0}C for 1 h followed by aging for 24 h. Finally, the obtained product was washed with distilled water, centrifuged and dried at 100 ^{0}C for 12 h and then calcined at 400 ^{0}C for 3 h.

Synthesis of HAp@Al_2O_3 core-shell NPs

The HAp@Al_2O_3 core–shell NPs were prepared by using sonochemical approach (Gedanken *et al*., 2004). In brief, aluminum isopropoxide (0.2 g) was dissolved in ethanol (60 ml) to form a clear solution. Then, 6 ml of HAp NPs (20 mg/ml) were added with the aid of ultrasonication for 20 min. After that, a 1:5 (v/v) mixture of water and ethanol (50 ml) was added, and the reaction mixture was ultrasonicated for another 2 h. The product was washed with ethanol for several times to remove the solvent and unbound aluminum isopropoxide. Finally, the HAp@Al_2O_3 core-shell NPs were vacuum dried at 80 ^{0}C overnight to gain the white powder. The dried powder was calcinated at 600 ^{0}C for 2 h.

Synthesis of gelatin coated HAp@Al_2O_3 core-shell NPs

The Al^{3+} ions of alumina shell were formed a covalent bond with R-COO^- ions of GEL molecules. In a typical experiment, 250 mg of gelatin was dissolved in hot Milli-Q wter (30 ml), and then 100 mg of core-shell HAp@Al_2O_3 NPs dispersed in ethanol (10 ml) were added. After stirring for 24 h, the gelatin coated NPs (HAp@Al_2O_3-GEL) were gathered through centrifugation at 12,000 rpm and washed with ethanol and water.

Synthesis of FA conjugated HAp@Al_2O_3-GEL NPs

Folic acid was conjugated with gelatin coated HAp@Al_2O_3 NPs via EDAC and NHS chemistry. In brief, 1 gm of folic acid was dissolved into 40 ml of Milli-Q water, and 0.84 gm of EDAC and 0.5 gm of NHS was added. The FA activation was carried out at room temperature for 3 h under dark condition. To the above activated folic acid solution, the solution of 0.5 gm of gelatin coated HAp@Al_2O_3 NPs in 10 ml of hot Milli-Q water was slowly added, the whole solution was stirred at room temperature for 24 h in dark. Finally the FA conjugated gelatine-HAp@Al_2O_3 core-shell NPs was obtained by centrifugation, washed several times with ethanol and water, and dried in a vacuum at 60 ^{0}C for 12 h.

Synthesis of drug loaded HAp@Al_2O_3-GEL-FA NPs

5 mg of 5-fluorouracil was dissolved in 5ml of Milli-Q water and then 10 mg of HAp@Al_2O_3-GEL-FA NPs was added in to drug solution, the solution was stirred at room temperature for 4 hrs, free drug was separated from the encapsulated drug into NPs using centrifugation.

Drug loading and entrapment efficacy

In addition, the drug loading content and entrapment efficacy was determined by the following equation:

$$\text{Drug loading contents (\%)} = \frac{\text{Weight of drug in NPs}}{\text{Weight of NPs taken}} \text{X } 100$$

$$\text{Drug entrapment efficacy (\%)} = \frac{\text{Weight of drug in NPs}}{\text{Weight of drug taken}} \text{X } 100$$

In-vitro drug release

In order to determine the drug release pro le 100 mg of the Drug loaded NPs was introduced into a screw capped glass bottle containing 50 ml of phosphate buffered saline (PBS, pH-6.3 and 7.4) medium at 37 °C under sterile condition. 5 ml of samples was taken by a pipette at a standard interval of 1 h and substituted immediately with 5 ml of fresh PBS medium, which was accounted for when calculating the amount released. The amount of release 5-fluorouracil (5-Flu) in the supernatant solution was measured by UV-visible spectrophotometer at a wavelength of 227 nm.

In-vitro cytotoxicity

The MTT assay is based on the ability of live but not dead cells to reduce a yellow tetrazolium dye to a purple formazan product. Cells were maintained in DMEM medium, supplemented with 10% Fetal Bovine Serum, at 37 ^{o}C in humidified atmosphere with 5% CO_2. The cells were plated in 96 well flat bottom tissue culture plates at a density of approximately 1.2X 10^4 cells/well and allowed to attach overnight at 37^{o}C. The medium was then discarded and cells were incubated with different concentrations of the samples (10, 20, 30, 40, 50, 60 µg/ml) for 24 h. After the incubation, medium was discarded and 100µl fresh medium was added with 10µl of MTT (5mg/ml). After 4 h, the medium was discarded and 100µl of DMSO was added to dissolve the formazan crystals. Then, the absorbance was read at 570 nm in a microtitre plate reader (Gedanken, 2004).

Cell survival was calculated by the following formula:

Viability % = (Test OD/ Control OD) X 100

Cytotoxicity % = 100 – Viability%

Characterization of NPs

Fourier transform infrared (FT-IR) spectra was measured on FTIR spectrometer (Bruker IFS 55, Fällanden, Switzerland), X-ray diffraction (XRD) patterns were taken from X'pert PRO PAN alytical diffractometer operating with (Cu (Kα), λ=1.5406A°) source, and high resolution transmission electron microscopy (HRTEM) photographs were taken using a JEOL JEM -3010 Electron microscope operating at 300 keV, the magnifying power used was 600 and 800k times.

RESULTS AND DISCUSSION

FTIR analysis

Fig (1a, b & c) shows the FTIR spectra of HAp, HAp@Al_2O_3, and HAp@Al_2O_3-GEL-FA NPs respectively. The characteristic peaks for $PO4^{3-}$ appear at around 563, 900-1200 cm^{-1}. Fig (1b) shows the peaks for Al-O-Al at around 881, 739 cm^{-1}. C=O stretching at 1693 cm^{-1} for the amide I, N-H bend at 1515 cm^{-1} for the amide II of gelatin. The shift of the 1339 cm^{-1} band in GEL has been effectively used to confirm the chemical bond formation between carboxyl ions in GEL and HAp@Al_2O_3 phases. During the process of GEL coating HAp@Al_2O_3 NPs, the Al^{3+} ions of alumina shell was formed a covalent bond with $R\text{-}COO^{-}$ ions of GEL molecules. The peak at 1488 cm^{-1} is assigned to Phenyl and pterin ring of folic acid, this peak was confirmed the folic acid was successfully conjugated onto surface of the HAp@Al_2O_3-GEL NPs (Socrates, 2001).

XRD analysis

The XRD pattern of the as prepared HAp and HAp@Al_2O_3 core-shell nanoparticles calcined at 400 ^{o} C for 3 h is shown in the Fig (2a & b). After calcination the powders reveal the crystallinity con rmation of HAp, and can be well indexed to hexagonal crystal structure, (ICDD Card le no. 9-432) (Socrates *et al*., 2001). The scintillation detector present in the instrument moves through the required angle at specific counts and scans the sample with a start angle at 10^{0} and a stop angle at 70^{0}. The output was obtained in the form of a graph with 2θ on x- axis and intensity on y-axis. From the result obtained, the average size of the nanoparticle was calculated using Scherer's formula,

$$\mathbf{D = 0.9\lambda / \beta \cos\theta}$$

Where β, λ and θ is full width at half maximum (FWHM) of the intensity, incident wavelength (for Cu (kα), λ=1.54056 A °) and reflection angle, respectively. The diffracted peaks correspond to hexagonal system that confirms the phase hydroxyapatite formation in Fig (2a) the peaks of HAp at 21 nm. The peaks of HAp and Al_2O_3 become more distinct and also new additional peaks of alumina at 23°, 50°, 53° and 66.5^{0} are observed in Fig (2b) and the particle size nearly 32 nm. These results indicate that the alumina reduces the crystallite size of HAp. Therefore, it is presumed that the introduction of alumina might affect crystalllinity of the HAp.

HR-TEM

The transmission electron microscopic analysis was carried out to confirm the particle size, growth pattern and distribution of crystallites. The HR-TEM image of HAp and alumina coated HAp NPs shown in Fig (3a, b, & c). The image indicated that the as prepared HAp powders was mono-dispersive and had a smooth surface and a rod-like shape, and the particle of diameter in the range of 21 nm was observed. The crystalline structures of the HAp NPs were further confirmed by selected-area electron diffraction (SAED) image investigations in Fig (3b). The HR-TEM image of alumina coated HAp NPs shown in Fig (3c) clearly displays the core– shell structure image of alumina coated HAp NPs, in which tinge shell is ascribed to alumina. A nearly well defined spherical morphology is observed and the HAp particles appear to be associated within Al_2O_3 shell. The boundary between the core HAp and the shell Al_2O_3 is very much distinct. This image illustrates that particle has a thin capping of Al_2O_3 shell of thickness in the range 15 nm.

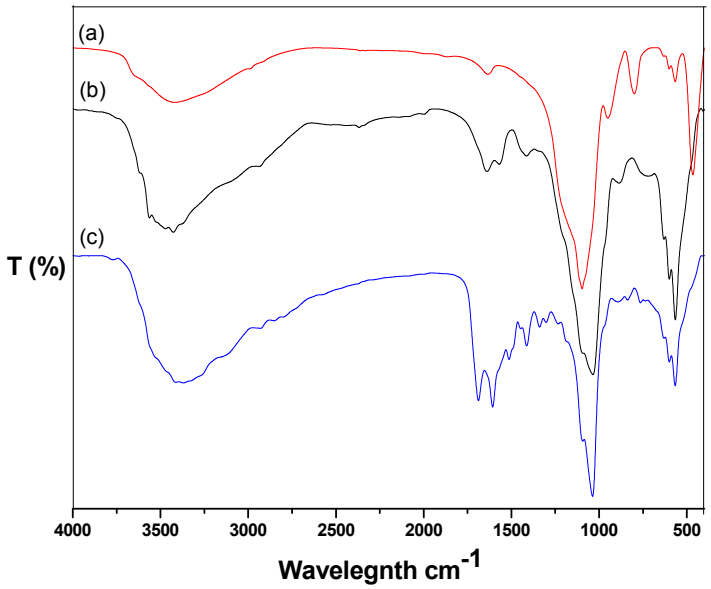

Fig. 1. FTIR-spectrum of (a) HAp (b) HAp@Al_2O_3 (c) HAp@Al_2O_3-GEL-FA NPs

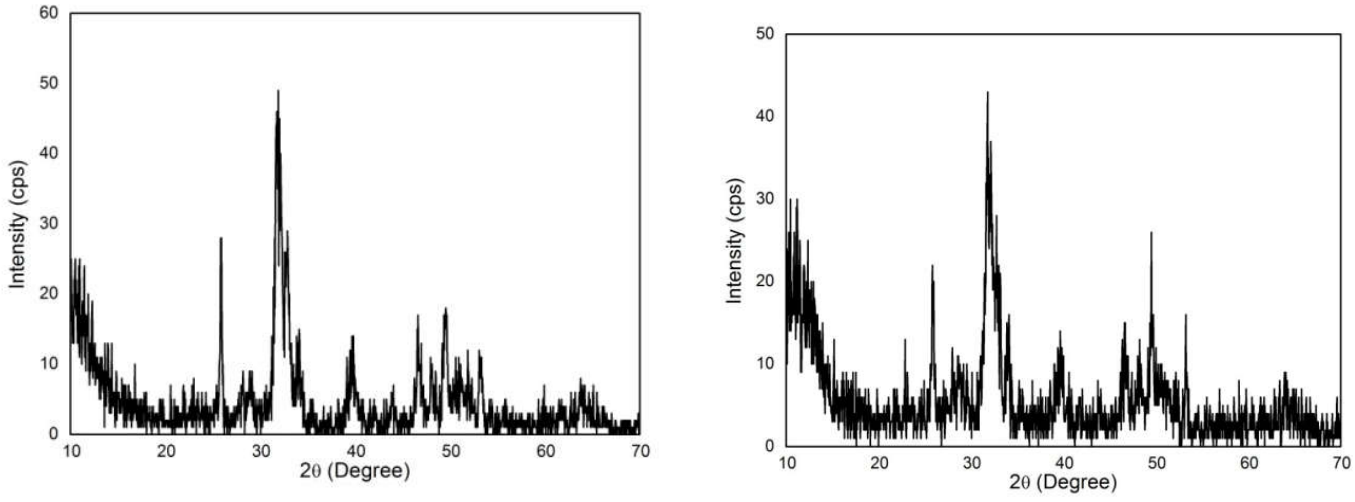

Fig.2. XRD patern of (a) HAp and (b) HAp@Al_2O_3 core-shell NPs

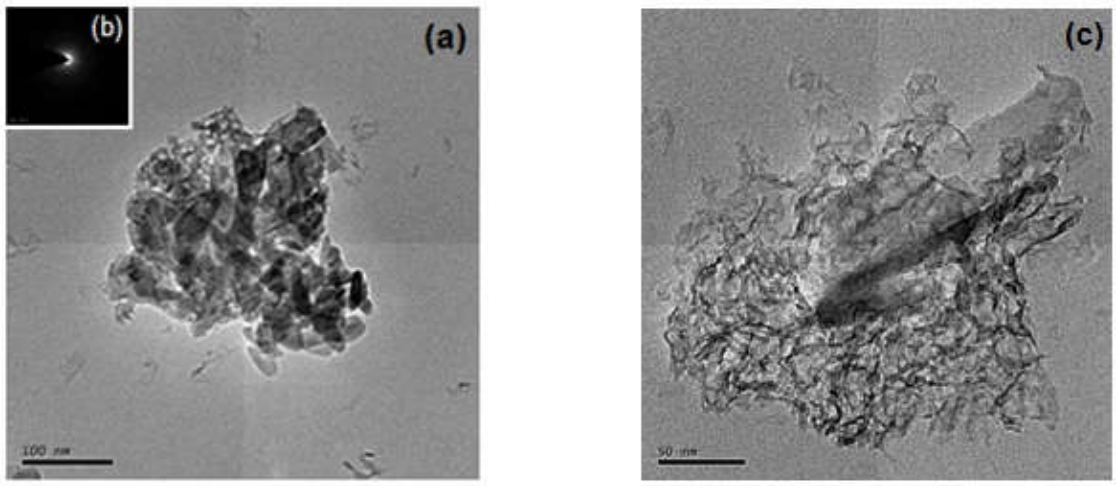

Fig.3. HR-TEM image of (a) HAp and (b) HAp@Al_2O_3 core-shell NPs

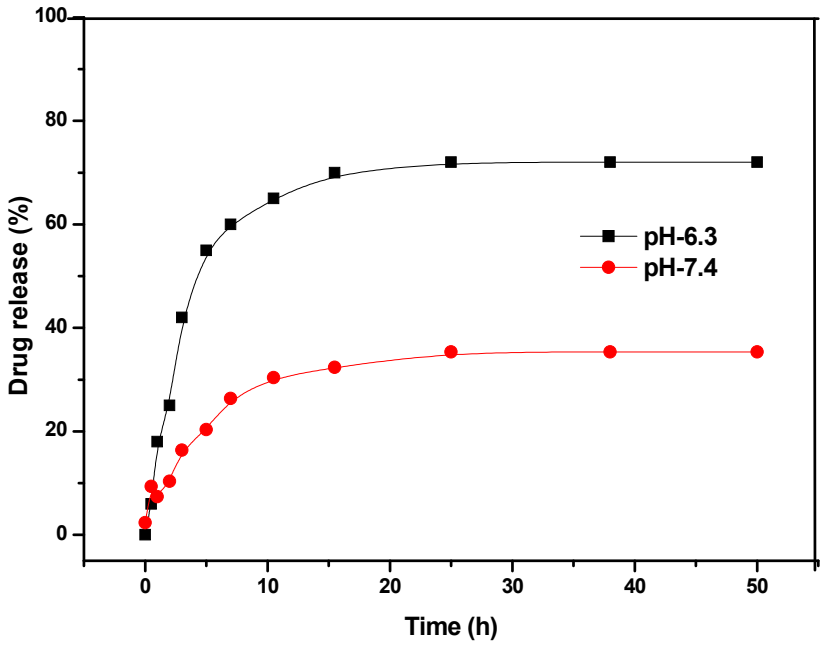

Fig.4. In-vitro drug release of 5-Flu loaded NPs at pH-7.4, and 6.3

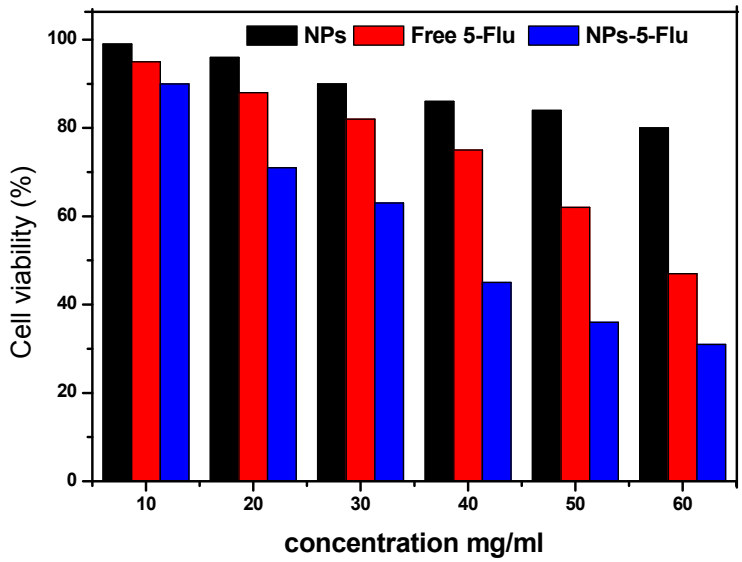

Fig.5. Cytotoxicity of free NPs, free 5-Flu, and 5-Flu loaeded NPs against with SKOV3 cell line

In-vitro drug release

The loading content and entrapment efficiency of 5-Flu in HAp@Al_2O_3-GEL-FA NPs are found to be 31.3% and 82.4% respectively. The amount of drug incorporated into HAp@Al_2O_3-GEL-FA measured by an UV–visible spectrophotometer. The drug release behaviour of 5-Flu loaded HAp@Al_2O_3-GEL-FA NPs was investigated in phosphate buffer at different pH conditions (PBS, pH-7.4 and 6.3). The drug release profiles of 5-Flu from the HAp@Al_2O_3-GEL-FA NPs are shown in Fig-4. This study clearly showed at pH 5.3 the amount released reached more than 60% within 7 h, and eventually reached to 60–72% after 43 h depending on the surface coating. In contrast, at pH 7.4 only 24% 5-flu was released within 7 h, and the equilibrium amount was about 33% in 50 h. This phenomenon can be mainly attributed to the larger degree of protonation of the carboxyl and amino groups at lower pH, which weakens the interaction between 5-Flu and HAp@Al_2O_3-GEL-FA NPs.

Cytotoxicity test

The cell viability of HAp@Al_2O_3-GEL-FA NPs, free drug, and drug loaded NPs were determined in the ovarian cancer cell line (SKOV3) using the MTT assay shown in Fig 5. The cytotoxicity of HAp@Al_2O_3-GEL-FA NPs, free 5-Flu, and 5-Flu loaded NPs were incubated with different concentrations (10, 20, 30, 40, 50, 60 µg/ml) for 24 h against a ovarian cancer cell line (SKOV3).

There was significant difference in cell viability incubation with HAp@Al_2O_3-GEL-FA NPs, free drug, and drug loaded NPs in SKOV3 cell line. Anticancer activity was more pronounced in the case of 5-Flu loaded NPs. Thus, the enhancement in the cytotoxicity of 5-Flu loaded HAp@Al_2O_3-GEL-FA NPs with the increase in concentration explicitly show more release of 5-Flu from the nanoparticles which induces cell death. These results demonstrate that the HAp@Al_2O_3-GEL-FA NPs could specifically increase the binding affinity for folate receptors thus, increase the viability of 5-Flu-HAp@Al_2O_3-GEL-FA NPs in SKOV3 cell line. The significant death of cancer cells due to the receptor mediated endocytosis caused by folate-receptors.

Conclusion

In summary, we prepared the targeted nanoparticulate drug delivery system functionalized with folic acid as the ligand for folate receptor over expressed in tumor cells and tumor endothelial cells. The Hydroxyapatite NPs was synthesized by co-precipitation method and HAp@Al_2O_3 core-shell NPs was prepared by sonochemical process. Gelatine and folic acid are attached onto the nanoparticles utilizing different techniques. HAp@Al_2O_3-gelatin-folic acid NPs were characterized by FTIR, XRD, and HR-TEM techniques. The drug release behaviour of 5-Flu loaded HAp@Al_2O_3-GEL-FA NPs was investigated in phosphate buffer at different pH conditions (PBS, pH-7.4 and 6.3), which exhibited a higher rate at pH 6.3 than at pH 7.4. The cytotoxicity of HAp@Al_2O_3-GEL-FA NPs, free 5-Flu, and 5-Flu loaded NPs was investigated in the ovarian cancer cell line (SKOV3) cell line using the MTT assay. 5-Flu loaded HAp@Al_2O_3-GEL-FA NPs shows greater cytotoxicity with SKOV3 cell line, due to the folate receptor mediated endocytosis. Therefore, these HAp@Al_2O_3-GEL-FA nanoparticles with high colloidal stability are promising candidates for targeted and enhanced intracellular delivery of anticancer drugs.

REFERENCES

Ansari MA, Khan HM, Khan AA, Cameotra SS, Saquib Q,Musarrat J 2014b. Interaction of Al2O3 nanoparticles with Escherichia coli and their cell envelope biomolecules. *J Appl Microbiol*.,116(4):772–783

Ansari MA, Khan HM, Khan AA, Pal R, Cameotra SS 2013. Antibacterial potential of Al2O3 nanoparticles against multi drug resistance strains of Staphylococcus aureus isolated from skin exudates. *J Nanopart Res*.

Bouyer E, Gitzhofer F, Boulos MI. 2000. Morphological study of hydroxyapatite nanocrystal suspension. *J Mater Sci Mater Med*., 11: 523-31

Capriotti L. A., T. P. Beebe and J. P. Schneider, 2007.Hydroxyapatite surface-induced peptide folding, J. *Am.Chem. Soc*., 129, 5281 5287.

Daniele RN, Lorena T, Montserrat M, Lourdes P, Rosa IM,Pilar V. 2013. In vitro 478 antitumor activity of methotrexate via pH-sensitive chitosan Nanoparticles. 479 *Biomat*., 34:2758–72.

Dubertret, B.; Skourides, P.; Norris, D. J.; Noireaux, V.; Brivanlou, A. H.; Libchaber, A. In vivo imaging of quantum dots encapsulated in phospholipid micelles. Science, 2002, 298, 1759–1762.

Evis Z., R.H. Doremus, 2005. Effect of Al2O3 Reinforcement and Al2O3–13 wt% TiO2 Bond Coat on Plasma Sprayed *Hydroxyapatite Coating Mater. Lett*., 59 3824.

Evis Z., R.H. Doremus, 2007. Hot-pressed hydroxylapatite/monoclinic zirconia composites with improved mechanical properties *J. Mater. Sci*., 42, 2426.

Fajardo C., M. L. Sacca, G. Costa, M. Nande and M. Martin, 2014. Impact of Ag and Al2O3 nanoparticles on soil organisms: In vitro and soil experiments Sci. *Total Environ*., 473–474, 254–261.

Fu L., A.K. Khiam, P.L. Joo, 2002. Effects of Yttria-Stabilized Zirconia on Plasma-Sprayed Hydroxyapatite/Yttria-Stabilized Zirconia Composite Coatings. *J. Am. Ceram. Soc*., 84 (4) 800.

Gautier S., E. Champion, D.B. Assollant, 1997. Processing, microstructure and toughness of Al2O3 platelet-reinforced hydroxyapatite. *J. Euro. Ceram. Soc*., 17; 1361.

Gedanken, A. 2004. Using Sonochemistry for the Fabrication of Nanomaterials. *Ultrason. Sonochem*, 11, 47–55.

Gordon T, Perlstein B, Houbara O, Felner I, Banin E, Margel S. 2011. Synthesis and characterization of zinc/iron oxide composite nanoparticles and their antibacterial properties. Colloids and Surfaces A: Physicochemical and Engineering Aspects., 374:1–8.

Guidi F., G. Moretti, G. Carta, M. Natali, G. Rossetto, Z.Pierino, G. Salmaso and V. Rigato, 2005. Electrochemical anticorrosion performance evaluation of Al2O3 coatings deposited by MOCVD on an industrial brass substrate Electrochim. *Acta*., 50, 4609–4614.

He L.P., M. Yui-Wing, Z.Z. Chen, 2004. Fabrication and characterization of nanometer CaP(aggregate)/Al2O3 composite coating on titanium, *Mater. Sci. Eng*., A 367, 51.

Im K.H., S.B. Lee, K.M. Kim, Y.K. Lee, 2007. Improvement of bonding strength to titanium surface by sol–gel derived hybrid coating of hydroxyapatite and titania by sol–gel process, *Surf. Coat. Technol*., 202, 1135.

Itokawa H., T. Hiraide, M. Moriya, M. Fujimoto, G. Nagashima, R. Suzuki, T. Fujimoto, 2007. A 12 month in vivo study on the response of bone to a hydroxyapatite polymethyl methacrylate cranioplasty composite, *Biomater*. 28, 4922-4927.

Jin, Y.; Jia, C.; Huang, S. W.; O'Donnell, M.; Gao, X. 2010. Multifunctional nanoparticles as coupled contrast agents. *Nat. Commun*., 1, 41.

Kantana W., P. Jarupoom, K. Pengpat, S. Eitssayeam, T. Tunkasiri, G. Rujijanagul, 2013. Properties of hydroxyapatite/zirconium oxide nanocomposites, *Ceram.Int*. 39, S379- S382.

Leo, E., Vandelli, M.A., Cameroni, R., Forni, F., 1997.Doxorubicin-loaded gelatin nanoparticles stabilized by glutaraldehyde: involvement of the drug in the crosslinking process. *Inter. J. Pharm*., 155, 75–82.

Li J., B. Fartash, L. Hermansson, 1995. Hydroxyapatite—alumina composites and bone-bonding Biomaterials, 16,417.

Liu X, Luo L, Ding Y, Xu Y 2011. Amperometric biosensors based on alumina nanoparticles-chitosan-horseradish peroxidase nanobiocomposites for the determination of phenolic compounds. *Analyst*, 136:696–701

M. Inuzuka, S. Nakamura, S. Kishi, K. Yoshida, K. Hashimoto, Y. Toda, K. Yamashita, 2004. Solid State Ionics 172, 509.

Mindivan H., C. Tekmen, B. Dikici, Y. Tsunekawa and M. 2009. *Gavgali, Mater. Des*., 30, 4516–4520.

Mohamed K.R., H.H. Beherei, G.T. EI Bassyouni, N. EI Mahallawy, 2013. Fabrication and mechanical evaluation of hydroxyapatite/oxide nano-composite materials, *Mater. Sci. Eng*., C 33, 4126-4132.

Monteiro-Riviere NA, Oldenburg SJ, Inman AO 2010. Interactions of aluminum nanoparticles with human epidermal keratinocytes. *J Appl Toxicol*., 30:276–285

Mossman, T. 1983. Rapid colorimetric assay for cellular growth and survival – application o proliferation and cytotoxicity assays. *J. Immunol. Methods*, 65: 55-63.

Nam, J. M.; Thaxton, C. S.; Mirkin, C. A. 2003. Nanoparticlebased bio-bar codes for the ultrasensitive detection of proteins. *Science*, 301, 1884–1886.

Pisarek M., A. Roguska, A. Kudelski, M. Andrzejczuk, M.Janik-Czachor and K. J. Kurzydłowski, 2013. *Mater. Chem.Phys*., 139, 55–65.

Rico A., P. Poza and J. Rodr´ıguez, 2013. High temperature tribological behavior of nanostructured and conventional plasma sprayed alumina-titania coatings. Vacuum, 88, 149–154.

Sadiq MI, Chowdhury B, Chandrasekaran N, Mukherjeem A 2009. Antimicrobial sensitivity of Escherichia coli to alumina nanoparticles. *Nanomedicine*., 5:282–286

Shixian L, Mingqiang L, Zhaohui T, Wantong S, Hai S, Huaiyu L, Xuesi C. 2013. 475 Doxorubicin-loaded amphiphilic polypeptide-based nanoparticles as an effi- 476 cient drug delivery system for cancer therapy. *Acta Biomat*., 9:9330–42. 477.

Singh D., M.D.L.C. Lorenzo-Martin, F. Gutiérrez-Mora, J.L. Routbort, E.D. 2006. Case, Acta Biomater., 2, 669. Skwarczynski M, Toth I 2011. Peptide-based subunit nanovaccines. *Curr Drug Deliv*., 8:282–289

Socrates, G. 2001. Infrared and Raman Characteristic Group Frequencies - Tables and Charts. 3. John Wiley & Sons Ltd;West Sussex, England.

Sudimack, J.; Lee, R. J. 2000. Targeted drug delivery via the folate receptor. *Adv*. *Drug Delivery Rev*., 41, 147–162.

Uyeda, R. 1991. Studies of ultrafine particles in Japan: crystallography. Methods of preparation and technological applications. *Prog Mater Sci*., 35:96

Veiseh, O.; Gunn, J. W.; Zhang, M. 2010. Design and fabrication of magnetic nanoparticles for targeted drug delivery and imaging. *Adv. Drug Delivery Rev*., 62, 284–304.

Wang Q., G. Shirong, Z. Dekun, 2005. Nano-mechanical properties and biotribological behaviors of nanosized HA/partially-stabilized zirconia composites, Wear 259, 952.

Wang, F.; Han, Y.; Lim, C. S.; Lu, Y. H.; Wang, J.; Xu, J.; Chen, H. Y.; Zhang, C.; Hong, M. H.; Liu, X. G. Simultaneous phase and size control of upconversion nanocrystals through lanthanide doping. Nature, 2010, 463, 1061–1065. (5)Q. Wang, G. Shirong, Z. Dekun, Wear 259 (2005) 952.

Yang Chun., Guo Ying-kui., Zhang Mi-lin, 2010. Thermal decomposition and mechanical properties of hydroxyapatite ceramic. *Trans. Nonferrous Met. Soc. China* 20, 254 258

Young, S., Wong, M., Tabata, Y., Mikos, A.G., 2005. Gelatin as a delivery vehicle for the controlled release of bioactive molecules. *J. Control. Rel*., 109, 256–274.

Zhang Y., L. Zhou, D. Li, N. Xue, X. Xu, J. Li, 2003. Oriented nano-structured hydroxyapatite from the template. *Chem. Phys. Lett*., 376, 493–497.

Zhang, Y.; Kohler, N.; Zhang, M. 2002. Surface modification of superparamagnetic magnetite NPs and their intracellular uptake. *Biomaterials*, 23, 1553–1561.

Zhou H., J. Lee, 2011. Nanoscale hydroxyapatite particles for bone tissue engineering, *Acta Biomater*., 7, 2769-2781.

****